Available online at www.sciencedirect.com
SCIENCE DIRECT
Physics Letters A 355 (2006) 331–336
PHYSICS LETTERS A
www.elsevier.com/locate/pla

Interior crises in quasiperiodically forced period-doubling systems

Woochang Lim, Sang-Yoon Kim *

Department of Physics, Kangwon National University, Chunchon, Kangwon-Do 200-701, Republic of Korea

Received 8 October 2005; received in revised form 15 December 2005; accepted 23 February 2006

Available online 10 March 2006

Communicated by A.R. Bishop

Abstract

As a representative model for quasiperiodically forced period-doubling systems, we consider the quasiperiodically forced logistic map, and investigate the dynamical mechanism for the interior crises. For small quasiperiodic forcing ε, a chaotic attractor abruptly widens via a "standard" interior crisis when it collides with a smooth unstable torus. However, as ε passes a threshold value, the smooth unstable torus loses its accessibility from the interior of the basin of the attractor. For this case, we use the rational approximation to the quasiperiodic forcing, and find that a nonstandard interior crisis occurs for a nonchaotic attractor (smooth torus or strange nonchaotic attractor) as well as a chaotic attractor when it collides with an invariant "ring-shaped" unstable set. Particularly, we note that a three-band smooth torus transforms into a single-band intermittent strange nonchaotic attractor through the nonstandard interior crisis. The intermittent strange nonchaotic attractor is also characterized in terms of the average interburst time and the local Lyapunov exponent.

PACS: 05.45.Ac; 05.45.Df; 05.45.Pq

Keywords: Quasiperiodically forced systems; Nonstandard interior crisis; Ring-shaped unstable set

1. Introduction

Dynamical transitions of attractors which occur with variation of the system parameters have been a topic of considerable interest. Particularly, sudden qualitative changes in the attractor are of special interest. Such discontinuous abrupt changes, called the crises, were first extensively studied in the logistic map [1] and two kinds of interior and boundary crises were discovered for the case of chaotic attractors. Here, we are interested in the interior crisis, through which an abrupt enlargement of a chaotic attractor occurs when it collides with an unstable periodic orbit which lies in the interior of the basin. Intermittent dynamics associated with the interior crisis has been well characterized in model systems [2] and in experiments [3].

In this Letter, we study the interior crisis in quasiperiodically forced period-doubling systems driven at two incommensurate frequencies. These dynamical systems have attracted much attention because of typical appearance of strange nonchaotic attractors (SNAs) which are strange (fractal) but nonchaotic (no positive Lyapunov exponent) [4]. Since the first description of SNAs by Grebogi et al. [5], dynamical behaviors of the quasiperiodically forced systems have been extensively investigated both theoretically [6–20] and experimentally [21]. In a recent work [14], Witt et al. investigated the interior crisis in the quasiperiodically forced logistic map, and found the appearance of an SNA via an interior crisis when the smooth unstable torus is inaccessible from the interior of the basin of the attractor due to the basin boundary metamorphosis [22]. However, the dynamical mechanism for the interior crisis, giving rise to the birth of an SNA, remains unclear because the unstable orbit inducing such an interior crisis was not explicitly located.

This Letter is organized as follows. In Section 2, we consider the quasiperiodically forced logistic map which is a representative model for quasiperiodically forced period-doubling systems, and study the dynamical mechanism for the interior crises by varying the nonlinearity parameter a of the logistic map and the quasiperiodic forcing amplitude ε. Interior crisis has been

* Corresponding author.
E-mail addresses: wclim@kangwon.ac.kr (W. Lim), sykim@kangwon.ac.kr (S.-Y. Kim).

0375-9601/$ – see front matter
doi:10.1016/j.physleta.2006.02.065

discovered first for the period-3 window in the (unforced) logistic map [1]. A period-3 window is opened through a saddle-node bifurcation creating a pair of stable and unstable period-3 orbits, and it is closed via an interior crisis where a chaotic attractor collides with the unstable period-3 orbit. Consequently, a sudden widening of the chaotic attractor occurs. We investigate the effect of quasiperiodic forcing on the interior crisis responsible for the disappearance of the period-3 window. For small ε, a standard interior crisis of a three-band chaotic attractor occurs through a collision with the smooth unstable torus (which is developed from the period-3 unstable orbit of the logistic map). However, as ε passes a threshold value, a basin boundary metamorphosis occurs, and then the smooth unstable torus loses its accessibility from the interior of the basin of the attractor. For this case, the type of the interior crisis changes. Using the rational approximation to the quasiperiodic forcing, it is found that a nonstandard interior crisis occurs for a non-chaotic attractor (smooth torus or SNA) as well as a chaotic attractor via a collision with an invariant ring-shaped unstable set [19]. Particularly, for the case of a three-band torus, the nonstandard interior crisis results in the birth of a single-band intermittent SNA. This intermittent SNA is also characterized in terms of the average interburst time and the local Lyapunov exponent. Finally, a summary is given in Section 3.

2. Interior crises in the quasiperiodically forced logistic map

We study the interior crises in the quasiperiodically forced logistic map M, often used as a representative model for the quasiperiodically forced period-doubling systems:

$$M: \begin{cases} x_{n+1} = (a + \varepsilon \cos 2\pi\theta_n) x_n (1 - x_n), \\ \theta_{n+1} = \theta_n + \omega \ (\mathrm{mod}\, 1), \end{cases} \tag{1}$$

where $x \in [0, 1]$, $\theta \in S^1$, a is the nonlinearity parameter of the logistic map, and ω and ε represent the frequency and amplitude of the quasiperiodic forcing, respectively. This quasiperiodically forced logistic map M is noninvertible, because its Jacobian determinant becomes zero along the critical curve, $L_0 = \{x = 0.5, \theta \in [0, 1)\}$. Critical curves of rank k, L_k ($k = 1, 2, \ldots$), are then given by the images of L_0 [i.e., $L_k = M^k(L_0)$]. Segments of these critical curves can be used to define a bounded trapping region of the phase space, called an "absorbing area", inside which, upon entering, trajectories are henceforth confined [23].

Here, we set the frequency to be the reciprocal of the golden mean, $\omega = (\sqrt{5} - 1)/2$. For the inverse golden mean, its rational approximants are given by the ratios of the Fibonacci numbers, $\omega_k = F_{k-1}/F_k$, where the sequence of $\{F_k\}$ satisfies $F_{k+1} = F_k + F_{k-1}$ with $F_0 = 0$ and $F_1 = 1$. Instead of the quasiperiodically forced system, we study an infinite sequence of periodically forced systems with rational driving frequencies ω_k. We suppose that the properties of the original system M may be obtained by taking the quasiperiodic limit $k \to \infty$. Using this technique, the mechanism for the interior crises is investigated.

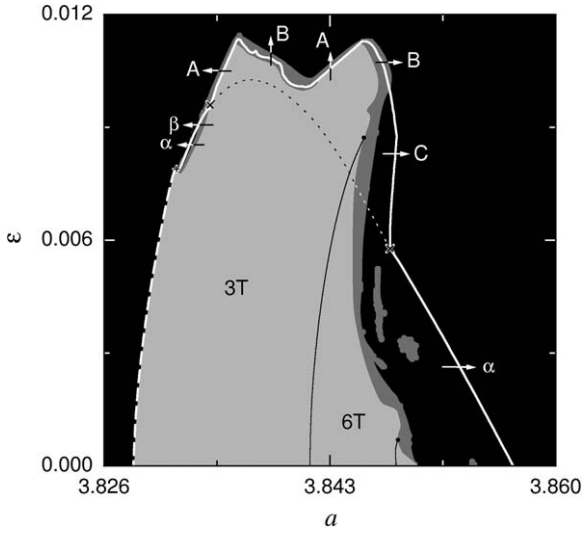

Fig. 1. Phase Diagram in the a–ε plane. Regular, chaotic, and SNA regimes are shown in light gray, black, and gray, respectively. For the case of regular attractor, a three-band torus exists in the region denoted by $3T$. When passing the solid line, a six-band torus appears in the region denoted by $6T$ via a torus-doubling bifurcation. (The terminal point of the torus doubling bifurcation curve is denoted by a solid circle.) An interior crisis occurs when crossing the white heavy line. This interior-crisis curve loses its smoothness at the two vertices (denoted by the crosses), and it ends at the terminal point (denoted by the plus) of the torus-collision bifurcation curve (represented by the white dashed line). When passing the dotted line, a basin boundary metamorphosis occurs, and then the smooth unstable torus becomes inaccessible from the basin of the attractor. For this case, a nonstandard interior crisis occurs along the routes A, B, and C through a collision with a ring-shaped unstable set. Such a nonstandard interior crisis is in contrast to the standard one occurring along the routes α and β via a collision with a smooth unstable torus. For other details, see the text.

Fig. 1 shows a phase diagram in the a–ε plane. Each phase is characterized by both the Lyapunov exponent σ_x in the x-direction and the phase sensitivity exponent δ. The exponent δ measures the sensitivity with respect to the phase of the quasiperiodic forcing and characterizes the strangeness of an attractor in a quasiperiodically driven system [8]. A three-band smooth torus has a negative Lyapunov exponent and no phase sensitivity ($\delta = 0$). Its region is denoted by $3T$ and shown in light gray. When crossing the black solid line, the three-band torus becomes unstable and bifurcates to a six-band torus in the region denoted by $6T$. On the other hand, chaotic attractors have positive Lyapunov exponents and its region is shown in black. Between these regular and chaotic regions, SNAs that have negative Lyapunov exponents and high phase sensitivity ($\delta > 0$) exist in the region shown in gray. Due to their high phase sensitivity, these SNAs have fractal structure. When crossing the white solid curve, an interior crisis where a three-band attractor transforms suddenly to an enlarged single-band attractor occurs. This interior-crisis curve starts from the interior-crisis point ($a = 3.8568$, $\varepsilon = 0$) of the logistic map and ends at the terminal point [represented by the plus (+)] of the torus-collision bifurcation curve (denoted by the white dashed curve) beginning from the saddle-node bifurcation point ($a = 1 + \sqrt{8}, \varepsilon = 0$) of the logistic map. When passing the white dashed curve, a three-band torus disappears through a

collision with a three-band unstable torus, and then a single-band intermittent chaotic attractor appears.

We first consider an interior crisis of a chaotic attractor which occurs along the route α for $\varepsilon = 0.002$ in Fig. 1. There exists a three-band chaotic attractor (denoted by black dots) with $\sigma_x = 0.14$ in the map M, as shown in Fig. 2(a) for $a = 3.85$. For this case, a smooth unstable three-band torus (denoted by the dashed line) lies near the chaotic attractor. As a increases and passes a threshold value of $a = 3.853\,760\,029$, the three-band chaotic attractor transforms suddenly to an enlarged single-band chaotic attractor through a collision with the unstable three-band torus. Thus, for $a = 3.855$, a single-band chaotic attractor with $\sigma_x = 0.578$ appears in M, as shown in Fig. 2(b). This interior crisis corresponds to a natural generalization of the interior crisis occurring for the unforced case ($\varepsilon = 0$). Hence, we call it the "standard" interior crisis.

As ε is increased, the standard interior-crisis line continues smoothly. However, at a lower vertex $(a_l^*, \varepsilon_l^*) \simeq (3.8475, 0.0058)$ (denoted by a cross in Fig. 1), the standard interior-crisis line ends and a nonstandard interior-crisis curve begins by making a sharp turning. Hence, the interior-crisis curve loses its differentiability at the vertex. For this case, the standard interior-crisis line is continued smoothly beyond the vertex as a curve of a basin boundary metamorphosis in the 3rd iterate of M (i.e., M^3) denoted by a dotted line. As the basin boundary metamorphosis line is passed, the basin boundary of an attractor in M^3 suddenly jumps in size [22]. We consider a smooth three-band torus in M, which exists below the basin boundary metamorphosis line. This three-band torus is transformed into the three tori in M^3. Fig. 2(c) shows the middle torus (represented by the heavy solid curve) inside its absorbing area bounded by the critical curves L_k ($k = 3, 6, 9, 12$) for $a = 3.84$ and $\varepsilon = 0.008$. The basin of the middle attractor is shown in light gray, while the basins of the upper and lower tori (not shown) are shown in gray. However, when passing the basin boundary metamorphosis line, the absorbing area becomes broken up through a collision with the smooth unstable torus (denoted by the dashed curve) on a basin boundary. Then, the basin of the middle torus becomes complex because it contains "holes" of other basins of the upper and lower tori, as shown in Fig. 2(d) for $a = 3.84$ and $\varepsilon = 0.01$ [24].

As a consequence of the basin boundary metamorphosis, the smooth unstable torus becomes inaccessible from the interior of basin of the middle torus, and hence it cannot induce any crisis. For this case, using the rational approximation to the quasiperiodic forcing, we locate an invariant ring-shaped unstable set that causes a nonstandard interior crisis through a collision with the smooth torus. Such a ring-shaped unstable set is born via a phase-dependent saddle-node bifurcation [19]. As an example, we consider the rational approximation of level $k = 5$ and explain the structure of the ring-shaped unstable set for $a = 3.84$. As shown in Fig. 2(e) for $\varepsilon = 0.00805$, the rational approximation to the smooth torus (denoted by the heavy solid curve), composed of stable orbits with period F_5 ($= 5$), exists. We also note that a ring-shaped unstable set, consisting of F_5 small rings, lies inside the basin. At first, each ring consists of the stable (shown in black) and unstable (shown in dark gray)

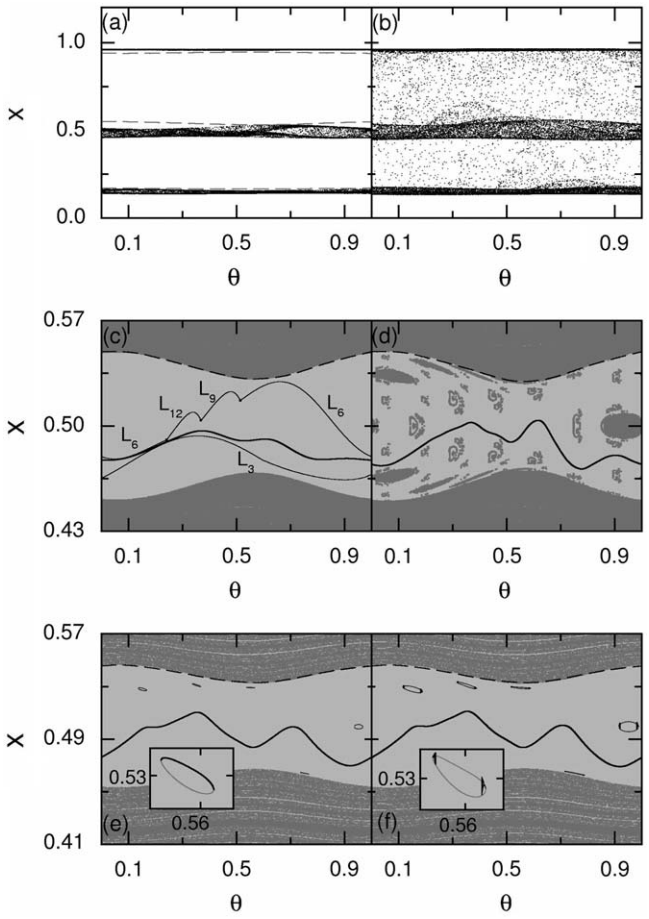

Fig. 2. (a), (b) Standard interior crisis of a chaotic attractor occurring along the route α for $\varepsilon = 0.002$. A smooth unstable torus (denoted by a dashed curve) lies near a three-band chaotic attractor (denoted by black dots) in (a) for $a = 3.85$. The three-band chaotic attractor transforms suddenly to an enlarged single-band chaotic attractor through a collision with the smooth unstable torus, as shown in (b) for $a = 3.855$. (c), (d) Basin boundary metamorphosis in the third iterate of M (i.e., M^3) for $a = 3.84$. A three-band torus in M turns into three tori in M^3. (c) A middle torus (denoted by a heavy solid curve) exists inside an absorbing area bounded by the critical curves L_k ($k = 3, 6, 9, 12$) in its basin (shown in light gray) for $\varepsilon = 0.008$. (d) "Holes" (denoted by gray dots), belonging to other basins of the upper and lower tori, appear inside the light gray basin of the middle torus for $\varepsilon = 0.01$ after breakup of the absorbing area. (e), (f) Appearance of a ring-shaped unstable set in the rational approximation of level 5 in M^3 for $a = 3.84$. A ring-shaped unstable set lies near the middle torus (denoted by the heavy solid line) for (e) $\varepsilon = 0.00805$ and (f) $\varepsilon = 0.0082$. A ring-shaped unstable set is composed of F_5 ($= 5$) small rings. Magnified views of a ring are given in the insets. Note that each ring consists of the unstable part (composed of unstable orbits with the forcing period F_5 and shown in dark gray) and the attracting part (denoted by black dots). For more details, see the text.

orbits with the forcing period F_5 [see the inset in Fig. 2(e)]. However, as ε is increased, such rings evolve, and thus each ring becomes composed of a large unstable part (shown in dark gray) and a small attracting part (denoted by black dots) [see Fig. 2(f) for $\varepsilon = 0.0082$]. As the level k of the rational approximation increases, the ring-shaped unstable set consists of a larger number of rings with a smaller attracting part. Hence, we believe that, in the quasiperiodic limit, the ring-shaped unstable set might become a complicated invariant unstable set composed of only unstable orbits. (For more details on the ring-

shaped unstable set, refer to Ref. [19].) Through a collision with this ring-shaped unstable set, a nonstandard interior crisis occurs, as will be shown below.

With further change in a and ε, both the nonstandard interior-crisis curve and the basin boundary metamorphosis line cease simultaneously at the upper vertex (denoted by a cross) $(a_u^*, \varepsilon_u^*) \simeq (3.8340, 0.0096)$ in Fig. 1. Then, the standard interior-crisis line, which joins smoothly with the basin boundary metamorphosis line at the upper vertex, starts again by making an angle. Along the routes α and β beyond the upper vertex, standard interior crises of the chaotic attractor and SNA occur, respectively. This standard interior-crisis curve ends at the terminal point (denoted by the plus) of the torus-collision bifurcation curve (represented by the white dashed line). Hereafter, we will investigate the nonstandard interior crises which occur along the routes A, B, and C crossing the segment bounded by the lower and upper vertices [see Fig. 1]. A nonstandard interior crisis is found to occur for a nonchaotic attractor [smooth torus (route A) and SNA (route B)] as well as a chaotic attractor (route C). Particularly, a single-band SNA appears as a result of the nonstandard interior crisis of a three-band smooth torus.

We fix the value of a at $a = 3.843$ and study the nonstandard interior crisis of a three-band smooth torus by varying ε along the route A. Fig. 3(a) shows a three-band smooth torus (denoted by solid curves) for $\varepsilon = 0.01$. As ε increases and passes

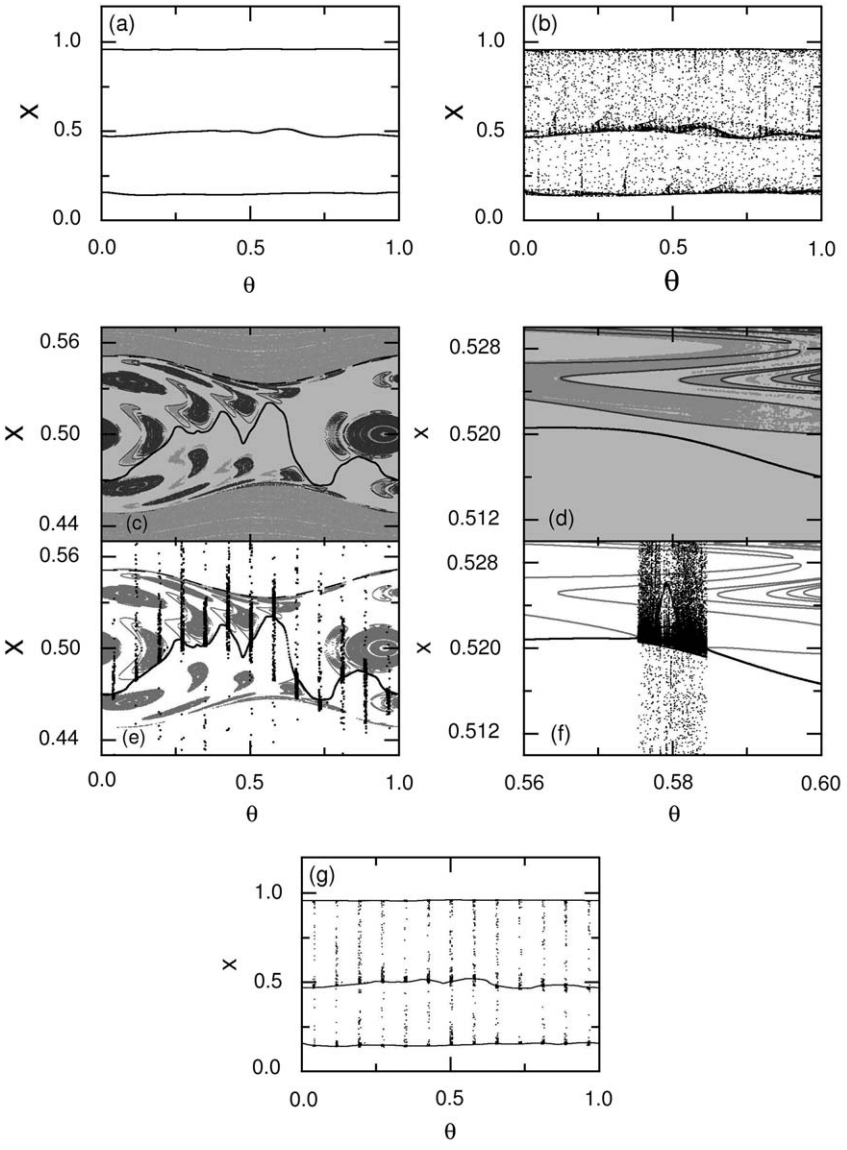

Fig. 3. (a), (b) Nonstandard interior crisis of a smooth three-band torus occurring along the route A for $a = 3.843$. (a) A three-band torus (denoted by the solid curve) for $\varepsilon = 0.01$. (b) An enlarged single-band SNA with $\sigma_x = -0.003$ and $\delta = 5.738$ for $\varepsilon = 0.010536$. (c)–(g) Analysis of the mechanism for the nonstandard interior crisis of the smooth torus in the rational approximation of level 7 in M^3 for $a = 3.843$. Magnified views near $(\theta, x) = (0.58, 0.52)$ in (c) and (e) are given in (d) and (f), respectively. Here, the middle torus (denoted by the heavy solid curve) exists in its light gray basin in (c) for $\varepsilon = 0.0103$. Some part of a ring-shaped unstable set (shown in dark gray) lies on a boundary of holes (shown in gray) of other basins of the upper and lower tori [see a magnified view in (d)]. Through a collision between the middle torus and the ring-shaped unstable set, F_7 (=13) gaps, where single-band intermittent chaotic attractors exist, are formed, as shown in (e) for $\varepsilon = 0.01033$ [see a magnified view in (f)]. The (partially-merged) rational approximation to the whole attracting set in M is given in (g).

a threshold value ε^* ($= 0.010\,535\,889$), the smooth torus transforms suddenly to an enlarged single-band SNA, as shown in Fig. 3(b) for $\varepsilon = 0.010\,536$. Using the rational approximation of level $k = 7$, we investigate the mechanism for this nonstandard interior crisis of the three-band smooth torus in M^3. Fig. 3(c) shows the middle torus (denoted by the heavy solid curve) in its basin (shown in light gray) in M^3 for $\varepsilon = 0.0103$. We note that the basin of the middle torus contains holes (shown in gray) of other basins of the lower and upper tori. Hence, the smooth unstable torus (denoted by a dashed curve) is not accessible from the interior of the basin of the middle torus. For this case, some part of a ring-shaped unstable set (shown in dark gray) lies on a hole boundary (e.g., see a magnified view in Fig. 3(d), where holes in the light gray basin are represented by gray dots). The rational approximation to the smooth torus and the ring-shaped unstable set are composed of the stable and unstable orbits with period F_7 ($= 13$), respectively. As ε is increased, the smooth torus and the ring-shaped unstable set on the hole boundary become closer, and eventually, for $\varepsilon = \varepsilon_7^*$ ($= 0.010\,325\,331$) a phase-dependent saddle-node bifurcation occurs through a collision between the smooth torus and the ring-shaped unstable set. Then, F_7 ($= 13$) "gaps", where the former attractor (i.e., the stable F_7-periodic orbits) no longer exists, are formed, as shown in Fig. 3(e) for $\varepsilon = 0.01033$. In these gaps, single-band intermittent chaotic attractors (denoted by black dots) appear [for a clear view, a magnified gap is given in Fig. 3(f)] as a result of the attractor-merging crises of the upper, middle, and lower tori in the gaps. Thus, the rational approximation to the whole attracting set in the original map M becomes composed of the union of the three-band periodic component and the single-band intermittent chaotic component, as shown in Fig. 3(g). Since the periodic component is dominant, the average Lyapunov exponent ($\langle \sigma_x \rangle = -0.083$) is negative, where $\langle \cdots \rangle$ denotes the average over the whole θ. Hence, the (partially-merged) 7th rational approximation to the attractor in Fig. 3(g) becomes nonchaotic, and resembles the single-band SNA in Fig. 3(b), although the level $k = 7$ is low. By increasing the level of the rational approximation to $k = 13$, we study the interior crisis of the three-band torus. It is thus found that the threshold value ε_k^*, at which the phase-dependent saddle-node bifurcation of level k (inducing attractor-merging crises in the gaps in M^3) occurs, converges to the quasiperiodic limit ε^* ($= 0.010\,535\,889$) in an algebraic manner, $|\Delta\varepsilon_k| \sim F_k^{-\alpha}$, where $\Delta\varepsilon_k = \varepsilon_k^* - \varepsilon^*$ and $\alpha \simeq 2.0$. As the level k of the rational approximation increases, the number of gaps, where phase-dependent attractor-merging crises occur, becomes larger, and eventually in the quasiperiodic limit, the rational approximation to the attractor has a dense set of gaps, filled by single-band intermittent chaotic attractors. Consequently, an intermittent single-band SNA, containing the ring-shaped unstable set, appears, as shown in Fig. 3(b). We note that the nonstandard interior crisis of a three-band torus results in the birth of a single-band intermittent SNA.

The intermittent SNA, born via the nonstandard interior crisis, may be characterized in terms of the average time between bursts and the local Lyapunov exponents [2,13–15]. A typical trajectory of the third iterate of M (i.e., M^3) spends a long stretch of time in the vicinity of one of the three former attractors (i.e., the upper, middle, and lower tori), then it bursts out from this region and comes close to the same or other former tori where it remains again for some time interval, and so on. In this way the trajectory irregularly jumps between the three former tori. For this case, the characteristic time τ is the average over a long trajectory of the time between bursts (i.e., jumps) [2]. As shown in Fig. 4(a) for $a = 3.843$, the average value of τ exhibits a power-law scaling behavior [14],

$$\langle \tau \rangle \sim (\varepsilon - \varepsilon^*)^{-\gamma}, \quad \gamma = 0.5 \pm 0.001. \tag{2}$$

Fig. 4(b) shows the plot of the Lyapunov exponent σ_x versus $\Delta\varepsilon$ ($= \varepsilon - \varepsilon^*$). We note that σ_x abruptly increases during the transition from torus to SNA, which is similar to the case of the intermittent route to SNA [13]. We also discuss the distribution of local (M-time) Lyapunov exponents σ_x^M, causing the sensitivity of the SNA with respect to the phase θ of the quasiperiodic forcing [8]. As an example, we consider the case of $a = 3.843$ and $\varepsilon = 0.010\,536$ and obtain the probability distribution $P(\sigma_x^M)$ of local (M-time) Lyapunov exponents σ_x^M by taking a long trajectory, dividing it into segments of length M, and calculating σ_x^M in each segment. For $M = 200$, 1000, and 2000, $P(\sigma_x^M)$'s are shown in Fig. 4(c). In the limit $M \to \infty$, $P(\sigma_x^M)$ approaches the delta distribution $\delta(\sigma_x^M - \sigma_x)$, where σ_x ($= -0.003$) is just the usual averaged Lyapunov exponent. However, we note that the distribution $P(\sigma_x^M)$ has a significant positive tail which does not vanish even for large M. To quantify this slow decay of the positive tail, we define the fraction of positive local Lyapunov exponents as

$$F_M^+ = \int_0^\infty P\left(\sigma_x^M\right) d\sigma_x^M. \tag{3}$$

These fractions F_M^+'s are plotted for $\varepsilon = 0.010\,536$, $0.010\,537$, and $0.010\,538$ in Fig. 4(d). Note that for each value of ε, the fraction F_M^+ exhibits a power-law decay,

$$F_M^+ \sim M^{-\eta}. \tag{4}$$

Here the values of the exponent η decreases as ε increases. Consequently, a trajectory on any SNA has segments of arbitrarily long M that have positive local Lyapunov exponents, and thus it has a phase sensitivity, inducing the strangeness of the SNA. As shown in Fig. 4(d), as ε increases the value of F_M^+ becomes larger. Hence, the degree of the phase sensitivity of the SNA increases.

As in the above case of a smooth torus (route A), a three-band SNA (chaotic attractor) transforms to a single-band one along the route B (C) in Fig. 1. Using the rational approximation to the quasiperiodic forcing, such a nonstandard interior crisis is also shown to occur through a collision with a ring-shaped unstable set.

3. Summary

We have investigated the mechanism for the interior crises in the quasiperiodically forced logistic map. Using the rational approximation to the quasiperiodic forcing, a nonstandard interior

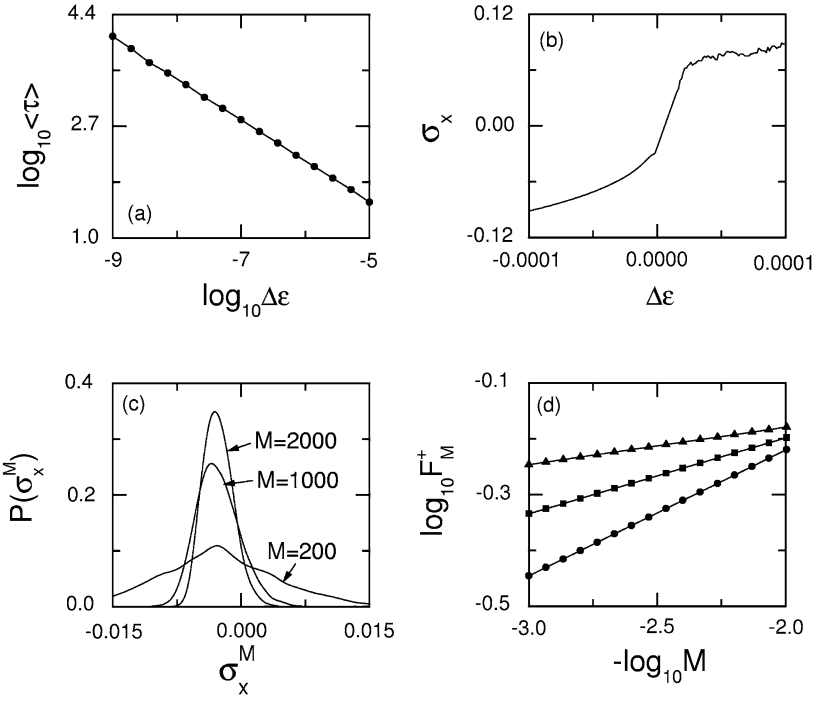

Fig. 4. (a) Plot of $\log_{10}\langle\tau\rangle$ ($\langle\tau\rangle$ is the average time between bursts) versus $\log_{10}\Delta\varepsilon$ ($\Delta\varepsilon = \varepsilon - \varepsilon^*$) for $a = 3.843$. The data are well fitted with the straight line with the slope $\gamma = 0.5 \pm 0.001$. (b) Plot of σ_x versus $\Delta\varepsilon$ for $a = 3.843$. We note an abrupt change in σ_x near the transition point. (c) Three probability distributions $P(\sigma_x^M)$ of the local M-time Lyapunov exponents for $M = 200$, 1000, and 2000 when $a = 3.843$ and $\varepsilon = 0.010536$. (d) Plots of $\log_{10} F_M^+$ (F_M^+: fraction of the positive local Lyapunov exponents) versus $-\log_{10} M$ for $a = 3.843$. Note that the three plots for $\varepsilon = 0.010536$ (circles), 0.010537 (squares), and 0.010538 (triangles) are well fitted with the straight lines with the slopes $\eta = 0.237$, 0.132, and 0.068, respectively. Hence, F_M^+ decays with some power η.

crisis has been found to occur for a nonchaotic attractor (smooth torus or SNA) as well as a chaotic attractor via a collision with an invariant ring-shaped unstable set. Particularly, a single-band intermittent SNA appears through the nonstandard interior crisis of a three-band smooth torus. Characterization of the intermittent SNA has also been made in terms of the average time between bursts and the local Lyapunov exponents. This kind of nonstandard interior crisis is in contrast to the standard interior crisis which occurs through a collision with a smooth unstable torus.

References

[1] C. Grebogi, E. Ott, J.A. Yorke, Phys. Rev. Lett. 48 (1982) 1507;
C. Grebogi, E. Ott, J.A. Yorke, Physica D 7 (1983) 181.
[2] C. Grebogi, E. Ott, F. Romeiras, J.A. Yorke, Phys. Rev. A 36 (1987) 5365;
C. Grebogi, E. Ott, J.A. Yorke, Phys. Rev. Lett. 57 (1986) 1284.
[3] W.L. Ditto, et al., Phys. Rev. Lett. 63 (1989) 923;
J.C. Sommerer, et al., Phys. Lett. A 153 (1991) 105.
[4] A. Prasad, S.S. Negi, R. Ramaswamy, Int. J. Bifur. Chaos 11 (2001) 291.
[5] C. Grebogi, E. Ott, S. Pelikan, J.A. Yorke, Physica D 13 (1984) 261.
[6] F.J. Romeiras, E. Ott, Phys. Rev. A 35 (1987) 4404;
M. Ding, C. Grebogi, E. Ott, Phys. Rev. A 39 (1989) 2593.
[7] J.F. Heagy, S.M. Hammel, Physica D 70 (1994) 140.
[8] A.S. Pikovsky, U. Feudel, Chaos 5 (1995) 253. See Eqs. (11)–(14) for the definition of the phase sensitivity exponent δ.
[9] O. Sosnovtseva, U. Feudel, J. Kurths, A. Pikovsky, Phys. Lett. A 218 (1996) 255.
[10] S.P. Kuznetsov, A.S. Pikovsky, U. Feudel, Phys. Rev. E 51 (1995) R1629;
S. Kuznetsov, U. Feudel, A. Pikovsky, Phys. Rev. E 57 (1998) 1585;
S.P. Kuznetsov, E. Neumann, A. Pikovsky, I.R. Sataev, Phys. Rev. E 62 (2000) 1995;
S.P. Kuznetsov, Phys. Rev. E 65 (2002) 066209.
[11] T. Nishikawa, K. Kaneko, Phys. Rev. E 54 (1996) 6114.
[12] T. Yalçınkaya, Y.-C. Lai, Phys. Rev. Lett. 77 (1996) 5039.
[13] A. Prasad, V. Mehra, R. Ramaswamy, Phys. Rev. Lett. 79 (1997) 4127;
A. Prasad, V. Mehra, R. Ramaswamy, Phys. Rev. E 57 (1998) 1576.
[14] A. Witt, U. Feudel, A. Pikovsky, Physica D 109 (1997) 180.
[15] A. Venkatesan, K. Murali, M. Lakshmanan, Phys. Lett. A 259 (1999) 246;
A. Venkatesan, M. Lakshmanan, A. Prasad, R. Ramaswamy, Phys. Rev. E 61 (2000) 3641;
A. Venkatesan, M. Lakshmanan, Phys. Rev. E 63 (2001) 026219.
[16] S.S. Negi, A. Prasad, R. Ramaswamy, Physica D 145 (2000) 1.
[17] H.M. Osinga, U. Feudel, Physica D 141 (2000) 54.
[18] B.R. Hunt, E. Ott, Phys. Rev. Lett. 87 (2001) 254101;
J.-W. Kim, S.-Y. Kim, B. Hunt, E. Ott, Phys. Rev. E 67 (2003) 036211.
[19] S.-Y. Kim, W. Lim, E. Ott, Phys. Rev. E 67 (2003) 056203;
S.-Y. Kim, W. Lim, J. Phys. A 37 (2004) 6477.
[20] S.-Y. Kim, W. Lim, Phys. Lett. A 344 (2005) 160.
[21] W.L. Ditto, M.L. Spano, H.T. Savage, S.N. Rauseo, J. Heagy, E. Ott, Phys. Rev. Lett. 65 (1990) 533;
T. Zhou, F. Moss, A. Bulsara, Phys. Rev. A 45 (1992) 5394;
W.X. Ding, H. Deutsch, A. Dinklage, C. Wilke, Phys. Rev. E 55 (1997) 3769;
T. Yang, K. Bilimgut, Phys. Lett. A 236 (1997) 494;
B.P. Bezruchko, S.P. Kuznetsov, Y.P. Seleznev, Phys. Rev. E 62 (2000) 7828.
[22] C. Grebogi, E. Ott, J.A. Yorke, Phys. Rev. Lett. 56 (1986) 1011;
C. Grebogi, E. Ott, J.A. Yorke, Physica D 24 (1987) 243.
[23] C. Mira, L. Gardini, A. Barugola, J.-C. Cathala, Chaotic Dynamics in Two-Dimensional Noninvertible Maps, World Scientific, Singapore, 1996.
[24] U. Feudel, A. Witt, Y.-C. Lai, C. Grebogi, Phys. Rev. E 58 (1998) 3060.